J Nanopart Res (2020) 22: 25
https://doi.org/10.1007/s11051-019-4734-8

RESEARCH PAPER

Core-shell structured carbon nanotubes/N-doped carbon layer nanocomposites for supercapacitor electrodes

Chong Xie · Shenghui Yang · Xuequan Xu · Jian-Wen Shi · Chunming Niu

Received: 8 July 2019 / Accepted: 11 December 2019 / Published online: 8 January 2020

Abstract N-Doped carbon layer–coated carbon nanotube (N-C/CNT) nanocomposites with stable core-shell structures were synthesized using a one-pot hydrothermal reaction. After high-temperature carbonization and KOH activation, the resultant N-C/CNT materials used as supercapacitor electrodes show high specific capacitance, good rate capability, and long cycle stability. The specific capacitance exhibits a high value of 322.1 F g^{-1} at 1 A g^{-1}, and still maintains 200.7 F g^{-1}, 168.7 F g^{-1}, and 120.0 F g^{-1} at 5 A g^{-1}, 10 A g^{-1}, and 20 A g^{-1}, respectively. During the 10,000-cycle testing at 5 A g^{-1}, the specific capacitance was kept stable. The high performance of the supercapacitor electrodes could be attributed to the synergistic effect of the high specific surface area with fine pore structure, high electronic conductivity, and mechanical strength of CNT support and pseudocapacitance provided by doping N atoms in the carbon layer.

Keywords Core-shell structure · Carbon nanotubes · Supercapacitor · Nitrogen doping · Nanomaterials

Introduction

Supercapacitors with a series of advantages compared with lithium-ion batteries, such as fast charge/discharge processes, high specific power, and long cycle life, have attracted persistent attention during the recent decades (Alaş et al. 2019; Genc et al. 2017; González et al. 2016; Han et al. 2018; Kasap et al. 2019; Lu et al. 2018; Najib and Erdem 2019; Repp et al. 2018; Tan et al. 2018). Supercapacitors can be divided into electrical double-layer capacitors (EDLCs) and pseudocapacitors based on different charge storage mechanisms. The former is based on electrostatic adsorption at the electrode/electrolyte interface, and the latter depends on the Faradaic reactions at the electrode/electrolyte surface (Peng et al. 2008).

The design of electrode materials is the key to determining the electrochemical performance of supercapacitors. Owing to the high specific surface area, relatively low cost, chemical stability, widespread resources, environment friendliness, etc., porous carbon materials such as activated carbons (ACs) are the most widely used electrode materials for supercapacitors. However, for ACs, there are still some disadvantages

Electronic supplementary material The online version of this article (https://doi.org/10.1007/s11051-019-4734-8) contains supplementary material, which is available to authorized users.

C. Xie · S. Yang (✉)
School of Materials Science & Engineering, Xi'an University of Technology, No. 5, South Jinhua Road, Xi'an 710048 Shaanxi, China
e-mail: yangsh@xaut.edu.cn

C. Xie · S. Yang · X. Xu · J.-W. Shi · C. Niu
Center of Nanomaterials for Renewable Energy, State Key Lab of Electrical Insulation and Power Equipment, School of Electrical Engineering, Xi'an Jiaotong University, Xi'an 710049, China

J.-W. Shi
e-mail: jianwen.shi@mail.xjtu.edu.cn

when used as supercapacitor electrode materials. For example, the porous structure with very less mesopores in the ACs limits the transfer of electrolyte ions during rapid charge/discharge processes resulting in poor rate capability. In addition, the activated process may introduce a large amount of structure defects in carbon networks, deteriorating the electrical conductivity (Deng et al. 2016; Borchardt et al. 2014; Zhang and Zhao 2009). As one allotrope of carbons, carbon nanotubes (CNTs) have high electrical conductivity, excellent mechanical strength, and a unique one-dimensional nanotubular structure (mesoporous structure). However, pure CNTs as capacitor electrode materials can only supply limited capacitance originating from the specific surface area (Niu et al. 1997; Futaba et al. 2006). Therefore, a design of AC/CNT nanocomposites combining the advantages of ACs and CNTs is a good strategy for supercapacitor electrode materials. However, because of the strong Van der Waals interaction among CNTs and the amphiphobic tubular surface of CNTs, it is difficult to disperse CNTs into a carbon matrix evenly or coat a carbon layer onto CNTs. Few papers were reported on the synthesis of well-designed AC/CNT nanocomposites, especially for the ACs/CNTs with a core-shell structure (Pan et al. 2016; Yao et al. 2015).

In addition, heteroatom-doped carbon, such as oxygen (Yu et al. 2017), nitrogen (Deng et al. 2016), and phosphorus (Wang et al. 2015), can improve capacitance significantly due to the additive Faradaic pseudocapacitance. Among the doped carbons, N-doped carbons have been recently demonstrated to be promising on improving the capacitance via surface Faradaic reactions without sacrificing the high rate capability and long cycle life (Deng et al. 2016). A certain amount of N atoms in carbon also can improve electronic conductivity and surface wetting (Hu et al. 2017; Liu et al. 2016). There have been two primary strategies to prepare N-doped carbons: direct thermal treatment of N-enriched carbon materials (polyaniline, polypyrrole, etc.) and post-treatment of carbon precursors with N-containing reagent (ammonia, urea, etc.) (Deng et al. 2016).

According to the aforementioned points, N-doped AC/CNT nanocomposites are used to realize high capacitance due to the synergistic advantages of ACs, CNTs, and N atom doping. However, until now, there are limited papers that reported facilely synthesizing N-doped carbon coating CNTs with core-shell structures as supercapacitor electrode materials (Yao et al. 2015). Herein, we designed N-doped carbon layer–coated CNT nanocomposites (N-C/CNTs) with core-shell structures as supercapacitor electrode materials using one-pot hydrothermal reaction, D-glucosamine hydrochloride as a natural carbon precursor, and nitrogen doping sources. After carbonization and activation, the resulting N-C/CNT nanocomposites exhibit high performance when used as supercapacitor electrodes, which could be attributed to the synergistic effect of the high specific surface area with fine pore structure, high electronic conductivity, and mechanical strength of CNT support and pesudocapacitance provided by the doping N atoms in the carbon layer.

Experimental section

Material synthesis

The CNTs were synthesized by chemical vapor deposition method. Before use, the as-prepared CNTs were soaked in a mixture solution of H_2SO_4 and $(NH_4)_2S_2O_8$ with a mole ratio of 1:1 for 14 days in order to introduce functional groups (–OH and –COOH) to the CNT surface. A total of 250 mg of functional CNTs was dissolved in 350 mL deionized water with ultrasonication for 1 h. Subsequently, 10 g D-glucosamine hydrochloride ($C_6H_{13}NO_5$·HCl) and 8 mL phytic acid (50 wt%) were added into the CNT dispersion under constant stirring. Then, the mixture dispersion was transferred into a stainless steel autoclave lined with polyphenylene (500 mL) and heated at 200 °C for 24 h under constant magnetic stirring. After hydrothermal reaction, the nanocomposites were separated by centrifugation and then dried by vacuum freeze-drying. The obtained nanocomposite was carbonized at 800 °C in Ar flow for 2 h at the rate of 3 °C/min. Finally, the carbonization product was activated under 800 °C in Ar flow for 30 min at the rate of 3 °C/min using KOH as activating agent, and the mass ratio of product and KOH is 1:6. The obtained material was soaked in HCl solution to remove the residual inorganic salt and then washed with deionized water until a neutral pH.

Material characterization

Scanning electron microscopy (SEM) images were obtained using an FEI Quanta 250 SEM (FEI, USA).

Transmission electron microscopy (TEM) was carried out using a JEM-2100 HT TEM (JEOL, Japan). The nitrogen adsorption-desorption isotherms were measured at 77 K using an Autosorb-iQ analyzer (Quantachrome, USA). Before the measurement, all samples were degassed at 100 °C for 6 h. Specific surface area was calculated by the BET method using the linear portion of the adsorption branch of the isotherms. Pore size and pore volume analyses were carried out with the BJH method using the desorption branch of the isotherms. X-Ray photoelectron spectroscopy (XPS) analysis was carried out with an AXIS Ultra OLD X-ray Photoelectron Spectrometer (Kratos Analytical, UK) operated at 150 W with Al Kα irradiation. Raman spectra were measured using a Renishaw Raman RE01 scope with a 514-nm excitation argon laser. The scan rate was 4 cm^{-1}.

Electrochemical characterization

Preparation of electrodes

The N-C/CNT powders were mixed with acetylene black and poly (tetrafluoroethylene) homogenized at a mass ratio of 8:1:1 in a mortar and pestle, and then the mixture was rolled into uniform thin films and punched into small pieces with a diameter of 14 mm. The pieces were pressed onto nickel foam with the same diameter and were used as working electrodes. And the mass loading of N-C/CNTs on each electrode was about 6 mg.

Electrochemical measurement

The electrochemical behaviors were tested using a three-electrode configuration on a CHI660E (Shanghai Chenhua, China) electrochemical workstation in 2 M KOH solution. Platinum foil and Ag/AgCl electrode were used as counter electrode and reference electrode, respectively. Cyclic voltammetry (CV) was carried out in the voltage range of − 0.9 V ~ − 0.15 V, with the scan rate from 5 to 50 mV s^{-1}. Electrochemical impedance spectroscopy (EIS) analysis was performed with the frequency in the range from 0.01 to 100 KHz and ac amplitude 5 mV. Galvanostatic charge-discharge tests were conducted at different current loads between approximately 1 and 20 A/g. The specific capacitances were calculated by the galvanostatic charge-discharge curves according to $It/m\triangle E$, where I is the charge-discharge current, t the discharge time, m the mass of activated materials, and $\triangle E$ the voltage.

Results and discussion

In order to improve the dispersibility and stability in H_2O, we introduced functional groups (such as –COOH, –OH) on the surface of CNTs. It is noted that stirring during the hydrothermal reaction is essential. In the previous experiments without stirring, although a part of D-glucosamine-derived carbons were evenly adsorbed on the surface of CNTs, most of the derived carbons formed carbon microspheres via self-assembly (Fig. A1). And it is difficult to remove carbon microspheres from products. Sevilla and Fuertes (2009) discussed the formation mechanism of carbon microspheres by hydrothermal carbonization of cellulose (glucose) in detail. When the concentration of hydrothermal-derived carbon in the reaction system reaches the critical supersaturation point, the derived carbons form the carbon microspheres via self-assembly. It is believed that the stirring process destroys the critical supersaturation point, compared with forming carbon microspheres; thus, the D-glucosamine-derived carbons would be preferably adsorbed on the surface of functional CNTs during the hydrothermal reaction.

Figure 1a shows the SEM image of as-prepared N-C/CNT products. The average diameter of N-C/CNTs is about 30 nm (Fig. A2). After carbonization (Fig. 1b) and KOH activation (Fig. 1c, d), the N-C/CNT nanocomposites with stable core-shell structures were obtained. The N-C/CNT nanocomposites maintain the one-dimensional tubular structure of CNTs. The thickness of the carbon layer on CNTs is about 10 nm (Fig. 1d). During carbonization, the D-glucosamine-derived carbon is converted into the graphitic carbon shell (Figure A3). Meanwhile, the decomposition of derived carbon releases some organic gas molecules and creates microporous structures in the graphitic carbon layer during the carbonization process (Figure A3b) (Yao et al. 2015), and the specific surface area is only 195.8 m^2/g (~ 384 m^2/g for pristine functional CNTs).

As electrode materials of supercapacitors, a larger specific surface area is beneficial for higher capacitance. Activated treatment is of importance for introducing more microporous structures into the carbon layer, as well as increasing the specific surface area. According to numerous attempts by using different activated

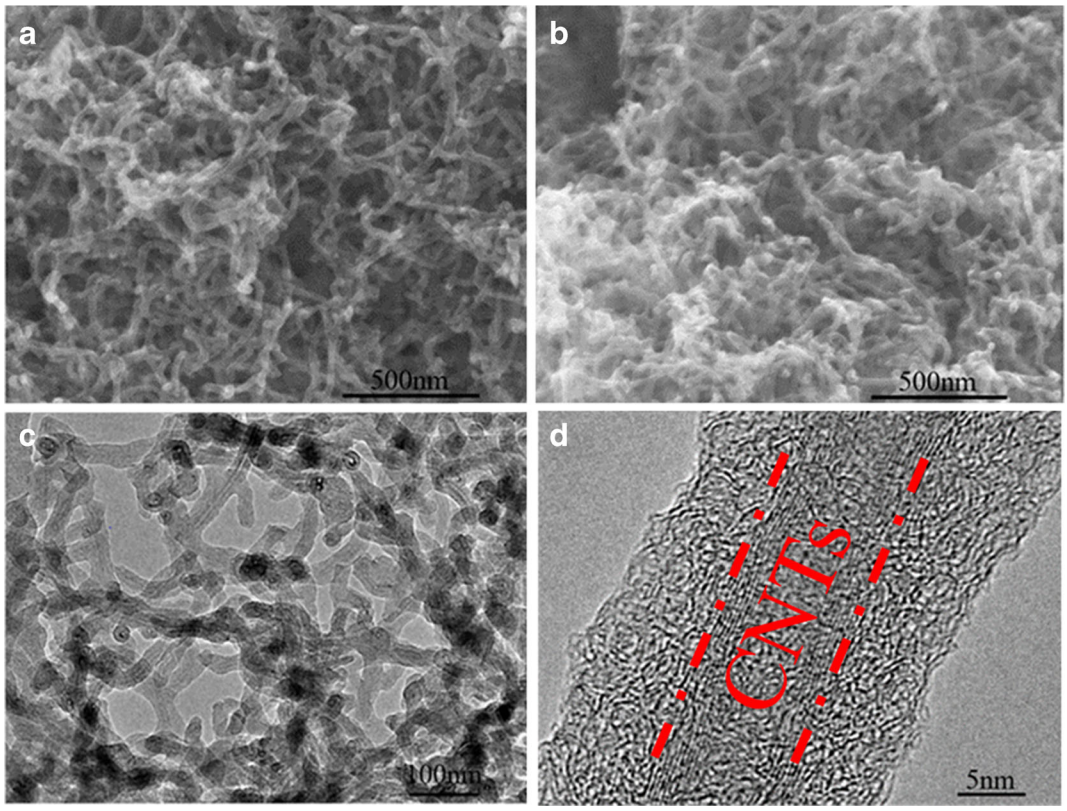

Fig. 1 **a** SEM image of as-prepared N-C/CNT nanocomposites. **b** SEM image of N-C/CNT nanocomposites after carbonization at 800 °C. **c** TEM image and **d** HRTEM image of N-C/CNT nanocomposites after KOH activation, respectively

strategies, KOH activation (Wang and Kaskel 2012) is an appropriate strategy without destroying the core-shell structure (Fig. 1d). Figure A4 exhibits the TEM image of the N-C/CNT materials after activated treatment by other methods. It is obvious that a part of derived carbons were exploited from CNT surface and the thickness of the carbon layer on CNTs was not uniform. Yao et al. (2015) also reported that wild KOH activation is more suitable for the C/CNT nanocomposite with a core-shell structure than the mild CO_2 activation.

Figure 2a shows the N_2 adsorption-desorption isotherm of N-C/CNTs after KOH activation. The isotherm shows a type H4 hysteresis loop according to the IUPAC classification (Kruk and Jaroniec 2001). Figure 2b exhibits pore volume and pore size distribution. The pore structure is mainly composed of micropores (< 2 nm), together with moderate mesopores, and the corresponding specific surface area is up to 1338 m^2/g, which is close to six times larger than that after carbonization. Compared with the carbonized sample, KOH activation introduces more micropores into the carbon layer, and the pore volume increases from 0.943 to 1.482 cm^3/g (Fig. 2b). Moreover, the mesopores in the composite were caused by the CNT support with nanotubular structures, which is beneficial for the rapid migration of the electrolyte ions. As capacitor electrode materials, a high specific surface area with fine pore size distribution is essential for excellent supercapacitor performance (Jia et al. 2017).

Figure 3a shows the full XPS spectrum of N-C/CNTs. Two stronger peaks at 284 eV and 527 eV can be assigned to C1s and O1s excitations, respectively (Xie et al. 2016a, b). A weak peak at 400 eV belongs to the N1 s (An et al. 2013; Wang et al. 2016). The atom percentages of C, O, and N are 88.43%, 9.41%, and 2.16%, respectively. The high-resolution N1s spectra can be fitted into two peaks (Fig. 3b), originating from graphitic N (400.8 eV) (An et al. 2013) and pyridinic N (398.9 eV) (Wang et al. 2016). And the concentrations of graphitic N atom and pyridinic N atom are 62.78% and 37.22%, respectively. According to the literature published before, graphitic N and pyridinic N in the carbon framework can enhance the electrical

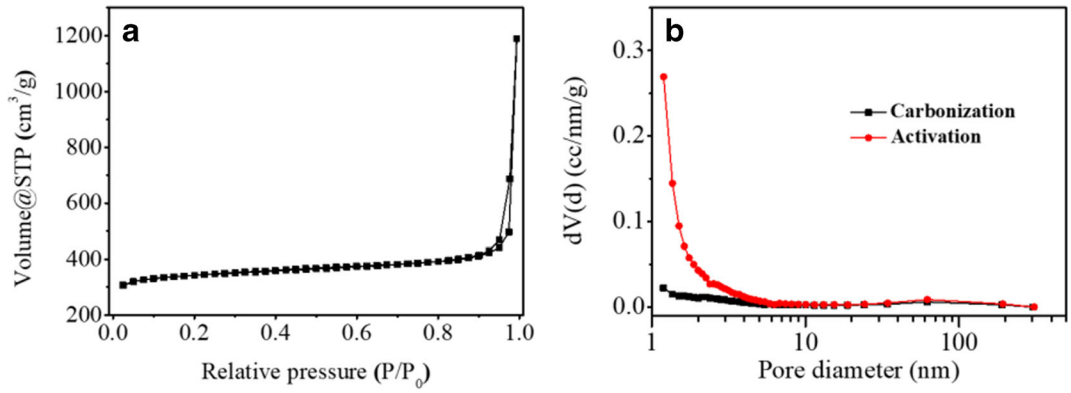

Fig. 2 **a** N_2 adsorption-desorption isotherm and **b** pore volume and pore size distribution of N-C/CNTs after KOH activation

conductivity and improve the surface wetting, respectively (Hu et al. 2017; Liu et al. 2016).

The electrochemical behaviors of N-C/CNT materials for supercapacitor electrodes were tested in 2 M KOH electrolyte with a three-electrode configuration. The Nyquist plot (Fig. A5) is composed of a semicircle at a high-frequency region and a nearly straight line at a low-frequency region, indicating ideal capacitive property. The equivalent series resistance (ESR) is only 1.3 Ω, which is attributed to the CNT support with high electrical conductivity. Figure 4a shows the CV curves at scan rates from 5 to 50 mV s^{-1}. The rectangular-like CV curves with two little humps indicated that the capacitance is composed of EDLC and pseudocapacitance from redox reaction. The CV curves still maintain the rectangular shape when the scan rate increases from 5 to 50 mV s^{-1}, except the reduction of humps. A transition region, corresponding to the redox reaction, was also observed in the galvanostatic charge/discharge curves (Fig. 4b). This phenomenon is related to the N atom doping in carbon materials, which is in good agreement with other literatures. Zhao et al. synthesized N-doped carbons by hydrothermal carbonization of D-glucosamine, and the similar humps appeared in CV curves and galvanostatic charge-discharge curves when used as capacitor electrode materials (Zhao et al. 2010). The specific capacitances are calculated by the galvanostatic charge-discharge curves. Figure 4c shows the specific capacitance as a function of current densities. The specific capacitance exhibits a high value of 322.1 F g^{-1} at 1 A g^{-1}, and still maintains 200.7 F g^{-1}, 168.7 F g^{-1}, and 120.0 F g^{-1} at 5 A g^{-1}, 10 A g^{-1}, and 20 A g^{-1}, respectively. The cyclic stability was tested at a current density of 5 A g^{-1}, and the result is shown in Fig. 4d. During the 10,000-cycle testing, the specific capacitance firstly increased gradually, and then was kept stable at around 214 F g^{-1}. Yao et al. synthesized a series of CNT/carbon nanocomposites with different thicknesses of carbon shell,

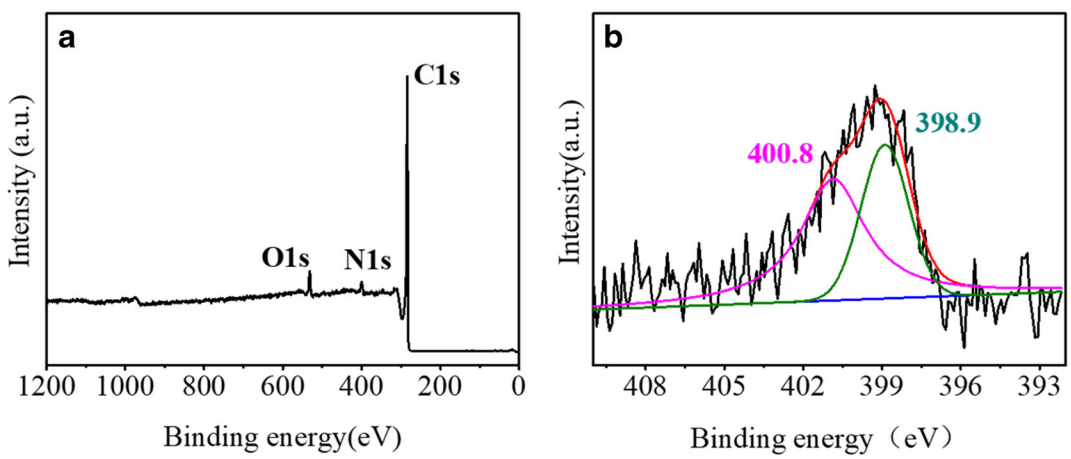

Fig. 3 **a** XPS spectrum and **b** the high-resolution N1s XPS of N-C/CNTs after KOH activation

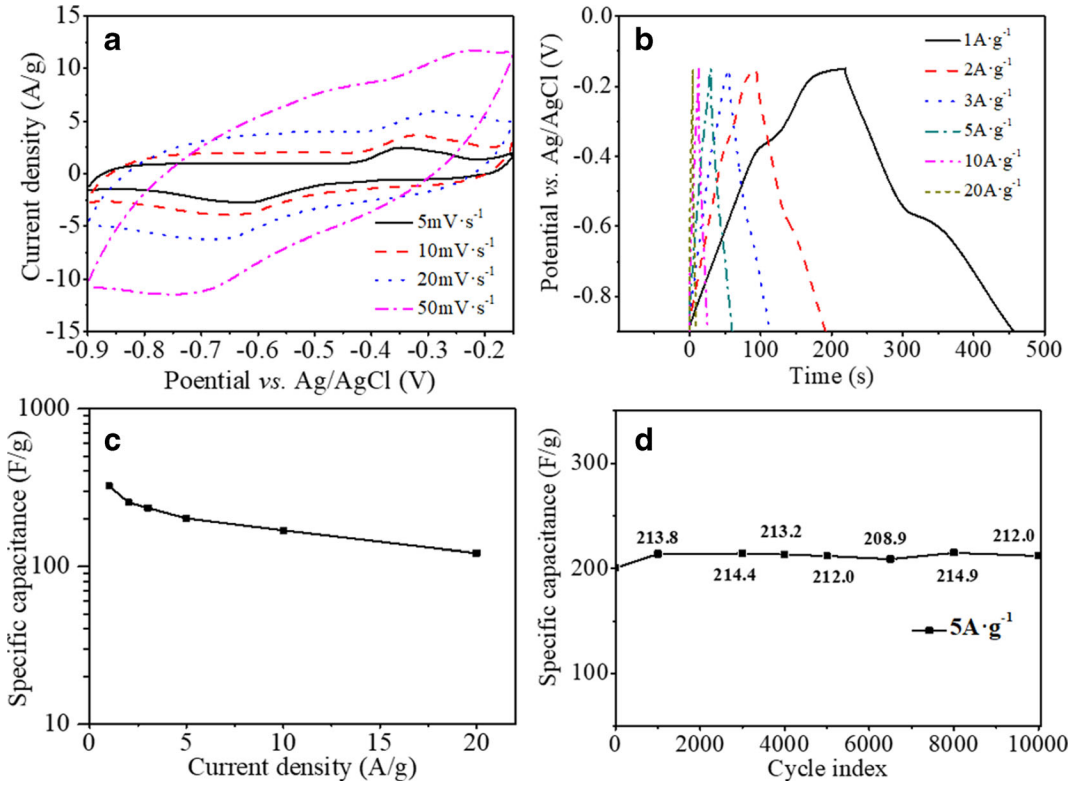

Fig. 4 **a** CV curves at different scan rates. **b** Galvanostatic charge/discharge curves at different current densities. **c** The specific capacitance as a function of current density. **d** Cycle performance at a current density of 5 A g^{-1}

and the results show that the capacitance retention slightly decreases with the thickness of activated carbon shell increasing (Yao et al. 2015). In this report, the thickness of the microporous carbon shell is about 10 nm. As a result, the N-C/CNTs exhibit excellent cyclic stability.

Conclusion

In summary, N-doped carbon layer–coated multi-walled carbon nanotube nanocomposite (N-C/CNTs) with stable core-shell structures were synthesized using a one-pot hydrothermal reaction successfully, followed by carbonization at high temperature and KOH activation. Stirring during the hydrothermal reaction process can avoid the formation of carbon microspheres. The resulting N-C/CNT nanocomposites have a core-shell nanostructure with CNT as the core and N-doped microporous carbon as the shell. The nanocomposites exhibit high specific capacitance and excellent cycle stability for supercapacitor electrodes. The high electrochemical performance could be attributed to the following aspects: (i) a high specific surface area with a fine-pore structure, which is mainly composed of micropores from the carbon shell, together with moderate mesopores from the three-dimensional network of CNTs; (ii) doping N atoms introduces Faradaic pseudocapacitance and improves specific capacitance significantly; (iii) as the skeleton (core) of the N-C/CNT nanocomposites, CNTs with high electrical conductivity and excellent mechanical properties could decrease the electrical resistance of electrodes, and maintain stability of physical structure during long cycle testing; (iv) the thickness of microporous carbon shell is several nanometers, which shortens the ions' paths within the microporous channels. The synthetic method and structural design in this work also can apply to other material systems.

Acknowledgments The SEM work was done at International Center for Dielectric Research (ICDR), Xi'an Jiaotong University, China. The authors also thank Ms. Yanzhu Dai for her help in using SEM.

Compliance with ethical standards

Conflict of interest The authors declare that they have no conflict of interest.

References

Alaş MÖ, Güngör A, Genç R, Erdem E (2019) Feeling the power: robust supercapacitors from nanostructured conductive polymers fostered with Mn^{2+} and carbon dots. Nanoscale 11: 12804–12816

An BG, Xu SF, Li LX, Tao J, Huang F, Geng X (2013) Carbon nanotubes coated with a nitrogen-doped carbon layer and its enhanced electrochemical capacitance. J Mater Chem A 1: 7222–7228

Borchardt L, Oschatza M, Kaskel S (2014) Tailoring porosity in carbon materials for supercapacitor applications. Mater Horiz 1:157–168

Deng YF, Xie Y, Zou KX, Ji XL (2016) Review on recent advances in nitrogen-doped carbons: preparations and applications in supercapacitors. J Mater Chem A 4:1144–1173

Futaba DN, Hata K, Yamada T, Hiraoka T, Hayamizu Y, Kakudate Y, Tanaike O, Hatori H, Yumura MT, Iijima S (2006) Shape-engineerable and highly densely packed single-walled carbon nanotubes and their application as super-capacitor electrodes. Nat Mater 5:987–994

Genc R, Alas MO, Harputlu E, Repp S, Kremer N, Castellano M, Colak SG, Ocakoglu K, Erdem E (2017) High-capacitance hybrid supercapacitor based on multi-colored fluorescent carbon-dots. Sci Rep 7:11222

González A, Goikolea E, Barrena JA, Mysyk R (2016) Review on supercapacitors: technologies and materials. Renew Sust Energ Rev 58:1189–1206

Han JW, Wei W, Zhang C, Tao Y, Lv W, Ling GW, Kang FY, Yang QH (2018) Engineering graphenes from the nano- to the macroscale for electrochemical energy storage. Electrochem Energy Rev 1:139–168

Hu JT, Yang J, Duan YD, Liu CK, Tang HT, Lin LP, Lin Y, Chen HB, Pan F (2017) The synergistic effect achieved by combining different nitrogen-doped carbon shells for high performance capacitance. Chem Commun 53:857–860

Jia DD, Yu X, Tan H, Li XQ, Han F, Li LL, Liu H (2017) Hierarchical porous carbon with ordered straightmicrochannels templated by continuous filamentglass fiber arrays for high performance supercapacitors. J Mater Chem A 5: 1516–1526

Kasap S, Kaya II, Reppc S, Erdem E (2019) Superbat: battery-like supercapacitor utilized by graphene foam and zinc oxide (ZnO) electrodes induced by structural defects. Nanoscale Adv 1:2586–2597

Kruk M, Jaroniec M (2001) Gas adsorption characterization of ordered organic-inorganic nanocomposite materials. Chem Mater 13:3169–3183

Liu L, Xu SD, Yu Q, Wang FY, Zhu HL, Zhang RL, Liu X (2016) The synergistic effect achieved by combiningdifferent nitrogen-doped carbon shells for high performance capacitance. Chem Commun 52:11693–11696

Lu J, Chen ZW, Pan F, Cui Y, Amine K (2018) High-performance anode materials for rechargeable lithium-ion batteries. Electrochem Energy Rev 1:35–53

Najib S, Erdem E (2019) Current progress achieved in novel materials for supercapacitor electrodes: mini review. Nanoscale Adv 1:2817–2827

Niu CM, Sichel EK, Hoch R, Moy D, Tennent H (1997) High power electrochemical capacitors based on carbon nanotube electrodes. Appl Phys Lett 11:1480–1482

Pan ZY, Ren J, Guan GZ, Fang X, Wang BJ, Doo SG, Son IH, Huang XL, Peng HS (2016) Synthesizing nitrogen-doped core–sheath carbon nanotube films for flexible lithium ion batteries. Adv Energy Mater 6:1600271

Peng C, Zhang SW, Jewell D, Chen GZ (2008) Carbon nanotube and conducting polymer compositesfor supercapacitors. Prog Nat Sci 18:777–788

Repp S, Harputlu E, Gurgen S, Castellano M, Kremer N, Pompe N, Wörner J, Hoffmann A, Thomann R, Emen FM, Weber S, Ocakoglu K, Erdem E (2018) Synergetic effects of Fe^{3+} doped spinel $Li_4Ti_5O_{12}$ nanoparticles on reduced graphene oxide for high surface electrode hybrid supercapacitors. Nanoscale 10:1877–1884

Sevilla M, Fuertes AB (2009) The production of carbon materials by hydrothermal carbonization of cellulose. Carbon 47:2281–2289

Tan SJ, Zeng XX, Ma Q, Wu XW, Guo YG (2018) Recent advancements in polymer-based composite electrolytes for rechargeable lithium batteries. Electrochem Energy Rev 1:113–138

Wang JC, Kaskel S (2012) KOH activation of carbon-based materials for energy storage. J Mater Chem 22:23710–23725

Wang J, Shen LF, Xu YL, Dou H, Zhang XG (2015) Lamellar-structured biomass-derived phosphorus- and nitrogen-co-doped porous carbon for high-performance supercapacitors. New J Chem 39:9497–9503

Wang CL, Zhang FF, Wang XX, Huang G, Yuan DX, Yin DM, Cheng Y, Wang LM (2016) Preparation of a graphitic N-doped multi-walledcarbon nanotube composite for lithium–sulfurbatteries with long-life and high specific capacity. RSC Adv 6:76568–76574

Xie C, Yang SH, Li BB, Wang HK, Shi JW, Li GD, Niu CM (2016a) C-doped mesoporous anatase TiO_2 comprising 10 nm crystallites. J Colloid Interface Sci 476:1–8

Xie C, Yang SH, Shi JW, Niu CM (2016b) Highly crystallized C-doped mesoporous anataseTiO_2 with visible light photocatalytic activity. Catalysts 6:117–127

Yao YY, Ma C, Wang JT, Qiao WM, Ling LC, Long DH (2015) Rational design of high-surface-area carbon nanotube/microporous carbon core-shell nanocomposites for supercapacitor electrodes. ACS Appl Mater Interfaces 7: 4817–4825

Yu MY, Xie BQ, Yang Y, Zhang Y, Chen Y, Yu WY, Zhang SS, Lu LH, Liu D (2017) Residual oxygen groups in nitrogen-doped graphene to enhance the capacitive performance. RSC Adv 7: 15293–15301

Zhang LL, Zhao XS (2009) Carbon-based materials as supercapacitor electrodes. Chem Soc Rev 38:2520–2531

Zhao L, Fan LZ, Zhou MQ, Guan H, Qiao SY, Antonietti M, Titirici MM (2010) Nitrogen-containing hydrothermal carbons with superior performance in supercapacitors. Adv Mater 22:5202–5206